Heat Pipe based Heat Exchanger Model

Basile Chaudoir

Year 2023-2024

Contents

Introduction

This document aims to present a thermosiphon heat exchanger model and give insights on the usability of this technology in the context of the DECAGONE project. This European project aims to recover heat from the flue gases of several types of industries. The recovered heat is meant to be converted into electricity using a cyclopentane ORC (Organic Rankine Cycle). In parallel, many studies also focus on improving the efficiency of ORCs by improving its components separately while reducing the required need for maintenance. The project could thus reduce waste heat across many industries, leading to an improvement of energy efficiency. One of the project tasks is to assess the potential of a recovery heat exchanger using the thermosiphon technology. This is the task that has been focused on in this report.

1 Presentation of Thermosiphon Technology

A thermosiphon is a technology that can be used as a passive heat exchanger. It consists in a shell (most simply a hollow tube) filled with a working fluid. This fluid can be chosen in order to fit better the application.

The tube is partly inserted in a heat source and another part is inserted in a heat sink (an adiabatic layer separates the two media). Reacting to the different temperatures of the media, evaporation takes place on the heat source side and condensation takes place simultaneously on the heat sink side. The evaporated working fluid flows in the middle of the tube while the condensed flows along the inner tube wall. This creates a latent heat displacement, allowing a high thermal conductivity of the thermosiphon tubes. The external fluid temperatures and flows impact the rates of evaporation and condensation, the tube adapts passively to these conditions and reaches an equilibrium. The equilibrium determines the saturation pressure inside the tube. This working principle is illustrated in Figure 1.

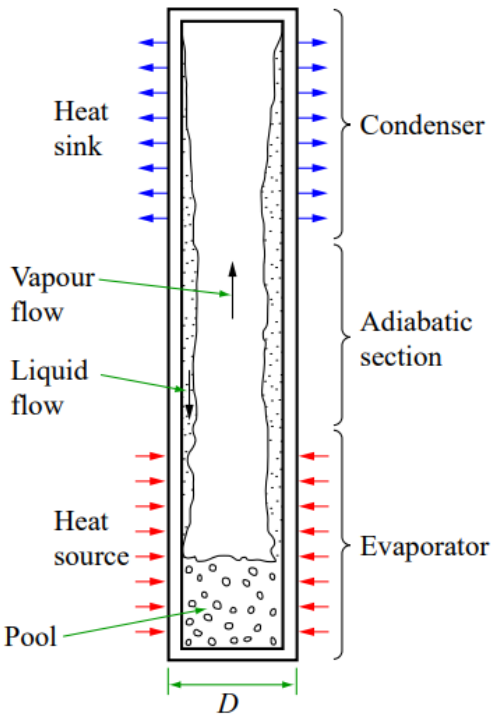

Figure 1: Thermosiphon sketch

2 Heat Pipe Model

This section aims to present the modelling of a thermosiphon bank interacting with the surrounding fluids. A thermosiphon is used as a thermal bridge between two media. It can be modelled in steady-state as a thermal resistance between the external fluids. In order to determine this thermal resistance, the latter is subdivided into many constitutive resistances based on the main thermal phenomena happening inside and outside the thermosiphon. This subdivision was done according to the ESDU model [1]. Figure 2 shows a representation of the main thermal resistances constituting the thermosiphon equivalent thermal resistance.

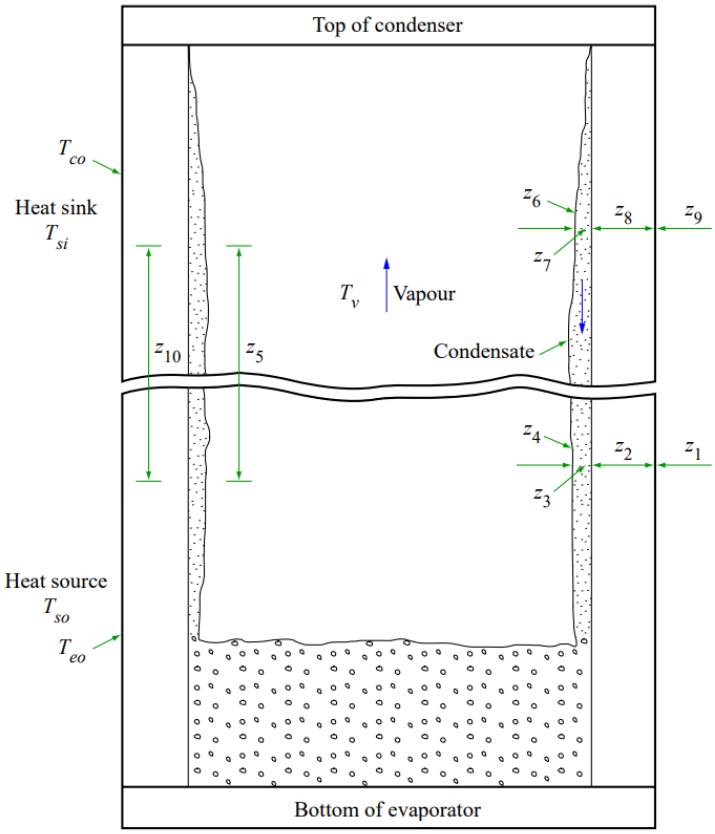

Figure 2: Model representation with thermal resistances

The equivalent thermal resistance can be modelled as represented in Figure 3. It can also be computed from its constituting sub-resistances as follows:

$$R_{th} = z_1 + \left[(z_2 + z_3 + z_4 + z_5 + z_6 + z_7 + z_8)^{(-1)} + z_{10}^{(-1)} \right]^{(-1)} + z_9 \tag{1}$$

The vapour/liquid interface related internal resistances (z_4 and z_6) were neglected as they are usually very small. Equation 1 becomes:

$$R_{th} = z_1 + \left[(z_2 + z_3 + z_5 + z_7 + z_8)^{(-1)} + z_{10}^{(-1)} \right]^{(-1)} + z_9 \tag{2}$$

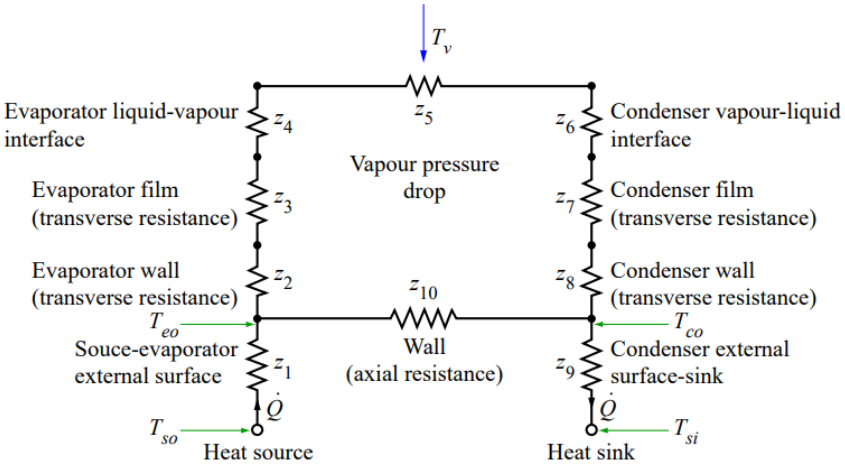

Figure 3: Thermal resistance bridge

The sub-resistances can be categorised into two types :

- Internal thermosiphon thermal resistances : $(z_2, z_3, z_5, z_7, z_8, z_{10})$. These are computed using the **HP_tube_model.py** and **HP_internal.py** files.
- Thermal resistances related to external fluids : (z_1, z_9). These are computed using the **HP_h_coeffs.py** file.

2.1 Thermosiphon Related Thermal Resistances

This subsection lists the resistances that are internal to the thermosiphon. These can be grouped in 3 sub-categories:

- Evaporation side resistances : (z_2, z_3).
- Condensation side resistances : (z_7, z_8).
- Axial resistances : (z_5, z_{10}).

2.1.1 Evaporation Side

The evaporation side resistances consists in:

- The evaporator wall (transverse resistance). This resistance is related to the conduction inside the thermosiphon wall and can be computed using the following equation:

$$z_2 = \frac{ln(D_o/D_i)}{2\pi l_e k_{pipe}} \tag{3}$$

  Where D_o and D_i are respectively the outer and inner diameters of the thermosiphon, l_e is the evaporation side length and k_{pipe} is the thermal conductivity of the thermosiphon wall material (steel).

- The evaporator film (transverse resistance). This resistance is composed of two parts. One is related to the liquid film along the evaporation part inner wall ($R_{film,e}$) and the second one is related to the liquid pool at the bottom of the evaporation side ($R_{pool,e}$).

R_{film} and R_{pool} can be respectively computed as follows [2] :

$$R_{film,e} = \frac{0.235\,\dot{Q}_{rad}^{(1/3)}}{D_i^{(4/3)}\,g^{(1/3)}\,l_e\,\phi_c^{(4/3)}} \quad with \quad \phi_c = \frac{\Delta h_e\,k_l^3\,\rho_l^2{}^{(1/4)}}{\mu_l} \tag{4}$$

$$R_{pool} = \frac{1}{\phi_e\,g^{(0.2)}\,\dot{Q}_{rad}^{(0.4)}\,(\pi\,D_i\,l_e)^{(0.6)}} \quad with \quad \phi_e = \frac{0.32\,\rho_l^{(0.65)}\,k_l^{(0.3)}\,cp_l^{(0.7)}}{\rho_v^{(0.25)}\Delta h_e^{(0.4)}\mu_l^{(0.1)}\,(P_{sat}/P_{atm})^{(0.23)}} \tag{5}$$

Where $\dot{Q}_{rad}$ is the thermosiphon radial heat flux (flowing from z_2 to z_8 in Figure 3, g is the gravity acceleration constant. ϕ_c and ϕ_e are respectively the figures of merit of water related to condensation and boiling.

The latter are computed using the liquid and gaseous fluid densities (ρ_l and ρ_v), the liquid thermal conductivity (k_l), thermal specific capacity (cp_l) and dynamic viscosity (μ_l). Other used properties are the specific boiling enthalpy (Δh_e) and the saturation pressure (P_{sat}).

Finally, the total resistance can be approximated as follows (where F_r is the filling ratio of the thermosiphon, usually fixed between 0.4 and 0.6):

$$z_3 = R_{pool} \qquad (\text{if } R_{pool} < R_{film})$$

$$z_3 = R_{pool}\,F_r + R_{film}\,(1 - F_r) \quad (\text{if } R_{pool} > R_{film})$$

- The evaporator liquid-vapour interface resistance (neglected here).

$$z_4 \approx 0 \tag{6}$$

2.1.2 Condensation Side

The condensation side resistances are modelled in a similar way as the evaporation side.

- The condenser wall (transverse resistance). This resistance is computed in a similar way as z_2 (see Equation 3):

$$z_8 = \frac{ln(D_o/D_i)}{2\pi l_c k_{pipe}} \tag{7}$$

  Here, l_c is the condensation side length.

- The condenser film (transverse resistance). As there is no liquid pool on the condenser side, this resistance consists only in the film resistance ($R_{film,c}$) that can be computed as follows:

$$z_7 = R_{film,c} = R_{film,e} = \frac{0.235\,\dot{Q}_{rad}^{(1/3)}}{D_i^{(4/3)}\,g^{(1/3)}\,l_c\,\phi_c^{(4/3)}} \quad with \quad \phi_c = \frac{\Delta h_e\,k_l^3\,\rho_l^2{}^{(1/4)}}{\mu_l} \tag{8}$$

  The different variables used have been enumerated under Equation 5.

- The condensation liquid-vapour interface resistance (also neglected here).

$$z_6 \approx 0 \tag{9}$$

2.1.3 Axial Thermal Resistances

The axial thermal resistances are the ones acting along the thermosiphon length:

- The wall axial resistance, which is the conduction resistance along the tube length:

$$z_{10} = \frac{l_{eff}}{k_{pipe}\, A_{axial}} \quad with \quad l_{eff} = l_a + \frac{l_e + l_c}{2} \quad and \quad A_{axial} = \frac{\pi}{4}(D_o^2 - D_i^2) \tag{10}$$

  Where l_{eff} is the thermosiphon effective length computed from the evaporation, condensing and adiabatic parts lengths (l_e, l_c and l_a). A_{axial} is the axial cross section computed from the internal and external pipe diameters (D_o and D_i).

- The vapour pressure drop related resistance. The pressure drop induces a temperature difference on both sides of the thermosiphon. It is computed as follows:

$$\begin{gathered} \Delta P = \frac{32\,\mu_v\,\dot{Q}_{rad}\,l_{eff}}{\rho_v\,A_v\,\Delta h_e\,D_v^2} \qquad (Re_a < 2300) \\ \Delta P = \frac{0.3164}{Re_a^{(1/4)}} \frac{\dot{Q}_{rad}^2\,l_{eff}}{2\,\rho_v\,A_v^2\,\Delta h_e^2\,D_v} \quad (Re_a > 2300) \\ A_v = \frac{\pi\,D_v^2}{4} \end{gathered} \tag{11}$$

  Where μ_v, ρ_v are respectively the vapour dynamic viscosity and density. Δh_e is the evaporation specific enthalpy, $\dot{Q}_{rad}$ is the radial heat transfer rate and Re_a is the flow Reynolds number. Finally, l_{eff} is the tube effective length and D_v is the vapour diameter (approximated as the tube internal diameter) and is used to compute A_v (the vapour cross section area).

2.2 External Fluids Thermal Resistances

This subsection lists the thermal resistances related to the external fluids. On the evaporation side (i.e the side where the water is evaporating in the thermosiphon), a flue gas flow in a tube bank was considered (thermodynamic properties of this gas were approximated as the ones for air). Concerning the condensation side, the resistance can take different values based on the configuration. Two cases were studied (these are represented in Figure 5:

- Case of oil (Therminol 66) flowing in a tube bank.
- Case of cyclopentane flowing and evaporating in a tube bank.

2.2.1 Evaporation Side - Flue gases

This subsection aims to provide correlations in order to compute z_1, the resistance between the flue gases and the thermosiphon wall. This also depends on the tube configuration that can be either inline or staggered.

The value of z_1 can be computed from the total heat transfer coefficient h_{fg} and the evaporation part area A_e. This coefficient is composed of a radiative $h_{fg,r}$ and a convective part $h_{fg,c}$.

$$z_1 = \frac{1}{A_e\,h_{fg}} = \frac{1}{A_e\,(h_{fg,r} + h_{fg,c})} \quad where \quad A_e = \pi\,l_c\,D_o \tag{12}$$

l_e is the condensation side length and D_o is the outer diameter of the thermosiphon.

Radiative Coefficient

The radiative coefficient can be computed as in Equation 13:

$$h_{fg,r} = 5.67 \times 10^{(-8)} \frac{(\varepsilon_{fg} T_g^4 - \alpha_{fg} T_w^4)}{T_g - T_w} \tag{13}$$

Where T_g is the flue gas temperature and T_w is the thermosiphon wall temperature. The flue gas emissivity ε_{fg} and absorptivity α_{fg} depend on the flue gas temperature and composition. They can be computed using empirical correlations as in [3].

Convective Coefficient

The convection coefficient can be computed from the flow Nusselt number (Nu), the fluid conductivity k and the pipe outer diameter D_o as for a tube bank [4] :

$$h = \frac{Nu\, k}{D_o} \tag{14}$$

The Nusselt Number can be computed itself as follows:

$$Nu = C\, Re_{max}^m\, Pr^{(0.36)} \left(\frac{Pr}{Pr_w}\right)^{(1/4)} \tag{15}$$

With:

- Pr and Pr_w being the flue gas Prandtl number and the flue gas Prandtl number at the thermosiphon wall,
- Re_{max} being the highest local Reynolds number in the tube bank (this happens between the first tubes). It is thus computed using the maximum flow velocity V_{max} that depends on geometrical parameters such as D_o and pitch ratios (parameter expressing the spacing between tubes) [cite tube banks, crossflow over],
- C and m being empirical coefficients depending on the tube bank configuration (inline or staggered) and on the Reynolds number. It is also to be noted that a coefficient C_2 can be added for tube banks with less than 20 rows in order to take into account the non-establishment of the flow across the bank.

Pressure drop

The pressure drop was also computed as the one of a tube bank:

$$\Delta P_{row} = \frac{1}{2}\, Eu\, \rho\, V_{max}^2 \tag{16}$$

Eu is the Euler coefficient and is computed using empirical correlations depending on the flow Reynolds number, the different pitch ratios and the tube bank configuration [5].

2.2.2 Condensation Side - Case of Circulating Oil Heating

This subsection aims to compute z_9 for the case of oil flowing across the thermosiphon tube bank. The thermal resistance and pressure drop are computed in a similar way as in last subsection (without taking into account the radiative part) by replacing flue gas properties by oil properties and by replacing l_c by l_e (length of evaporation zone) when computing the exchange surface area.

2.2.3 Condensation Side - Case of Cyclopentane Forced Convection Boiling

For this case, two types of heat transfer have to be considered in order to compute the heat transfer coefficient :

- Sensible heat is exchanged : The cyclopentane is not evaporating and the heat transfer coefficient can be computed as in Section 2.2.1.
- Latent heat is exchanged : The cyclopentane is evaporating during its flow.

For the case related to evaporation, the heat transfer coefficient can be computed using a correlation of Lienhard and Eichhorn [4] for external forced convection boiling in cross-flow over a tube.

This correlation computes the maximum heat flux across the surface $q"_{max}$ by distinguishing two cases:

- Low velocity flow which takes place if :

$$\frac{1}{\pi}\left[1+\left(\frac{4}{We_D}\right)^{1/3}\right] \geqslant \left[\frac{0.275}{\pi}\left(\frac{\rho_l}{\rho_v}\right)^{1/2}+1\right] \quad \text{where} \quad We_D = \frac{\rho_v V^2 D_o}{\sigma} \tag{17}$$

  We_D is the Weber number, ratio of inertia to surface tension forces. In this case, $q"_{max}$ can be computed as follows:

$$\frac{q"_{max}}{\rho_v \Delta h_e V} = \frac{1}{\pi}\left[1+\left(\frac{4}{We_D}\right)^{1/3}\right] \tag{18}$$

- Otherwise, high velocity flow is considered :

$$\frac{q"_{max}}{\rho_v \Delta h_e V} = \frac{(\rho_l/\rho_v)^{3/4}}{169\pi} + \frac{(\rho_l/\rho_v)^{1/2}}{19.2\pi\, We_D^{1/3}} \tag{19}$$

From $q"_{max}$, the related heat transfer coefficient h_{cb} was approximated :

$$h_{cb} = \frac{q"_{max}}{T_{w,c,o} - T_{c,o}} \tag{20}$$

$T_{w,c,o}$ and $T_{c,o}$ are respectively the outside wall temperature of the thermosiphon in the cold fluid part and the cyclopentane temperature.

From the value of the heat transfer coefficient h_{cb}, the thermal resistance can be computed in a similar way as in Equation 12 by replacing l_c by l_e (length of evaporation zone).

3 Heat Pipe Limits

3.1 ESDU Operation Limits

This section aims to list all operation limits of a thermosiphon that can be found in the ESDU standards [1].

- Entrainment limit ($\dot{Q}_{ent}$) : Even when there is sufficient liquid present in the thermosiphon to prevent dry-out occurring, the overall rate of heat transfer is subject to another limit; this occurs when the rate of entrainment of liquid by the vapour prevents the downward flow of liquid. This phenomenon puts a limit on the heat rate that can be computed as follows:

$$\dot{Q}_{ent} = F_1\, F_2\, F_3\, \Delta h_e\, \rho_v^{(1/2)}\, (\sigma g\, |\rho_l - \rho_v|)^{(1/4)} \tag{21}$$

  Where the $F_1\, F_2\, F_3$ group can be called Kutateladze number, the different constituting factor can be computed using adimensional correlations depending on the Bond number (Bo), an adimensional pressure parameter (K_p) and the thermosiphon inclination (β). This limits also depends on the evaporation enthalpy (Δh_e), the liquid and vapour densities (ρ_l and ρ_v), the liquid surface tension (σ) and the gravity acceleration constant (g).

- Boiling limit ($\dot{Q}_{boil}$) : Boiling limit occurs when a stable film of vapour is formed between the liquid and the heated wall of the evaporator. This stable film acts as an insulation and thus blocks the heat transfer. The associated limited can be computed as in Equation 22

$$\dot{Q}_{boil} = 0.12\, \rho_v\, \Delta h_e \left(\frac{\sigma |\rho_l - \rho_v|\, g}{\rho_v^2} \right)^{(1/4)} \tag{22}$$

- Sonic limit ($\dot{Q}_{son}$) : At low operating pressures, the vapour velocity may be appreciate compared with the sonic velocity in the vapour. This could create a sonic shock in the thermosiphon if the heat transfer rate were to be higher than the following limit.

$$\dot{Q}_{son} = 0.474\, \Delta h_e\, (\rho_v\, P_{sat})^{(1/2)} \tag{23}$$

  Where P_{sat} is the internal fluid saturation pressure.

- Dryout limit ($\dot{Q}_{dry}$) : As applied to thermosiphons, the term "dryout" implies that the volume of the liquid fill is not sufficient to cover all of the pipe above the pool with a film of liquid. Thus with a vertical pipe, most of the falling film of liquid would have evaporated before reaching the pool, leaving dry patches, with a few rivulets of liquid returning to the pool; with an inclined pipe, dry patches would appear at the top of the evaporator. The available evidence suggest that dryout in a vertical thermosiphon is avoided if the volume of liquid fill meets the conditions called for in ESDU 81038 Section 2.3.

$$\dot{Q}_{dry} = (2\, (\Delta h_e^2)\, \sigma\, \rho_v)^{(3/7)} \left(\frac{\rho_l |\rho_l - \rho_v|\, g\, \Delta h_e}{3 * \mu_l * l_e} \right)^{(1/7)} \left(\frac{F_r}{(447 * (1 - F_r)} \right)^{(4/7)} \tag{24}$$

  Where μ_l is the liquid dynamic viscosity, l_e the evaporation side length and F_r is the thermosiphon filling ratio.

- Vapor pressure limit ($\dot{Q}_{vap}$) : When operating a thermosiphon at a pressure substantially below atmospheric, the pressure drop of the vapor may be significant compared to the pressure in the evaporator. Vapor pressures are low but necessarily exceed zero at temperature close to the bottom of the operational range of a heat pipe. The minimum vapour pressure, which occurs at the closed end of the condenser, can be very small. The pressure drop in the vapour duct, ΔP_v, is then constrained by this effectively zero pressure and by the low vapour pressure existing at the closed end of the evaporator. Because ΔP_v increases with the overall rate of heat transfer, the constraint on ΔP_v requires $\dot{Q}$ (if not otherwise limited) to be approximately limited to a value, called the vapour limit.

$$\dot{Q}_{vap} = \frac{D_i^2 \, \Delta h_e \, P_{sat} \, \rho_v}{64 \, \mu_v \, l_e} \tag{25}$$

3.2 Limits on Working Fluid Saturation Pressure

This subsection aims to define the range of thermosiphon internal pressure in which the application can take place. This can also give some insight on some sizing parameters of the tubes. These can be defined by limits on the saturation pressure ($P_{sat,wf}$) in the thermosiphon:

- First, this pressure shall be lower than the critical pressure of the working fluid ($P_{c,wf}$) as a supercritical fluid does not allow any phase change, limiting the transfered heat to almost only pure conduction.

$$P_{sat,wf} < P_{c,wf} \tag{26}$$

- Secondly, the saturation pressure shall also be higher than the saturation pressure related to the temperature of the cold fluid. This ensures that the temperature inside the thermosiphon is higher than the one of the cold fluid so that the thermosiphon can operate.

$$P_{sat,wf} > P_{sat,wf}(T = T_{cf}) \tag{27}$$

- Finally, the pressure inside the thermosiphon shall be lower than the acceptable maximum pressure required for the integrity of the tubes (P_{max}). A too high pressure inside the thermosiphon could cause tube buckling and thus failure.

$$P_{sat,wf} < P_{max} \tag{28}$$

  P_{max} can be computed according the ASME BPVC [cite]. This can be computed for tubes and welded headers:

$$P_{max,tube} = S_{tube} \frac{2t - 0.01D_o - 2e}{D_o - (t - 0.005D_o - e)} \quad ; \quad P_{max,head} = \frac{4.8 \, t \, S_{tube}}{5D_i} \tag{29}$$

  Where S_{tube} is the maximum allowable stress with respect to temperature (for A-106C steel), D_o is the outer tube diameter, t is the tube wall thickness, e is the thickness factor for expanded tube ends (= 0 in this case) and D_i is the internal tube diameter. Note that $P_{max,head}$ is computed here for a hemispheric header with same thickness as the tube.

Some hypothesis were made for the computations of these maximum allowable pressures. For example, S_{tube} is temperature dependant and the worst case was chosen (i.e. it has been computed for the critical temperature of water about 373.15 $^\circ C$). t was also arbitrarily set to 3.5 mm. D_o was then varied from 18 to 58 mm and D_i was computed from its value and t. Figure 4 shows the results in terms of D_o

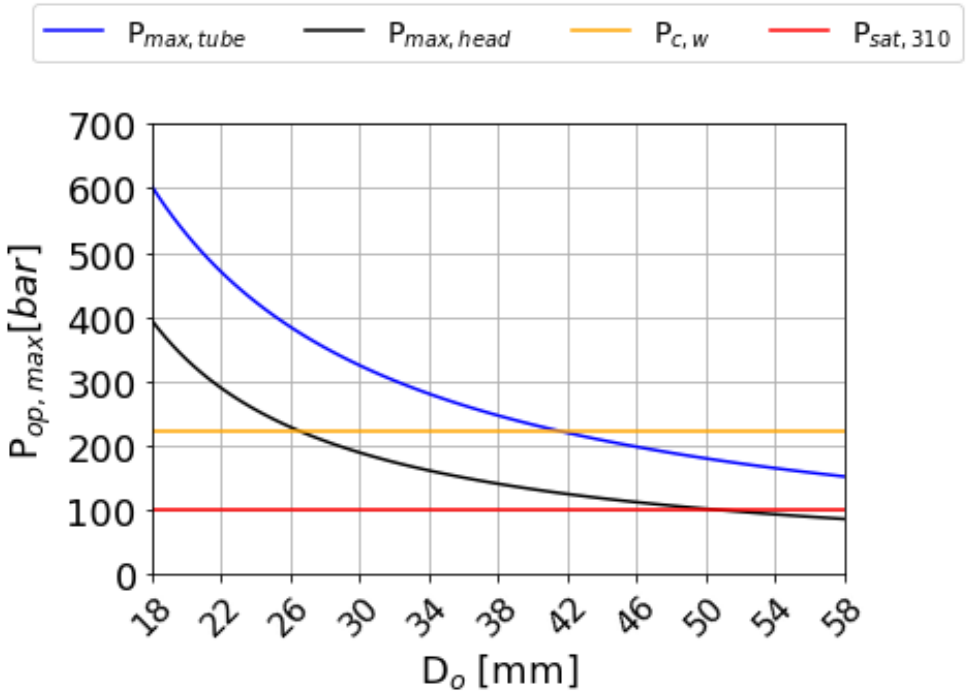

Figure 4: Limits on thermosiphon internal pressure depending on its outer tube diameter

In Figure 4, it can be seen that tubes outer diameter shall be lower than 50 mm because the maximum allowable pressure is equal to the saturation pressure of water at 310 $°C$. This means that the thermosiphon could not heat the oil at that temperature beyond that point without risk of buckling. Also, it shows that tubes of less than 26 mm of outer diameter can withstand the critical pressure of water. These tubes could cover all the possible application range of the thermosiphon technology. From 26 mm to 50 mm of outer diameter, the tubes have to be simulated in order to determine their operating pressure and if they can withstand them. Note that in the case of direct heating of cyclopentane to evaporate it at 240 $°C$, the associated water saturation pressure is of 33.47 $bars$. The tubes could then face much lower internal pressure and this limit would have less impact on the possible design and operation of the tubes.

3.3 Limits on Working Fluid Saturation Temperature

Another limit has been put arbitrarily for safety reasons. The maximum water temperature in the tube (i.e. the temperature in the first row on the flue gas side) shall not exceed 350 $°C$. This limit puts a security margin from the critical temperature of water. The critical temperature of water shall not be reached as the phase change could not happen beyond. This could lead to increase of the working fluid temperature and pressure that could cause tube failure. This also allows to reduce the maximum pressure inside the thermosiphon.

4 Tube Bank Model - General Hypothesis

The model as presented until now represents only one tube. In order to model a tube bank, many assumptions were done:

- Identical conditions for all tubes of a same row. This means that all tubes are computed in the same way and that the row heat transfer rate ($\dot{Q}_{row}$) equals the heat transfer rate of a tube ($\dot{Q}_{tube}$) multiplied by the number of tube per row (N_{tpr}):

$$\dot{Q}_{row} = \dot{Q}_{tube}\, N_{tpr} \tag{30}$$

- From one row to another, the inlet condition of the n+1 row is the outlet condition of the n row. The pressure drop is then computed row per row and cumulated.

$$P_{f,n+1} = P_{f,n} - \Delta P_n \tag{31}$$

- Many parameters where set for the sake of simplicity of the simulations:
  - The transversal (S_T) and longitudinal (S_L) pitch ratios also have been considered as the same.
  - The tube configuration of the bank is inline. A staggered configuration would show slightly better results but inline configuration are easier to maintain and clean up.

- The width of the exchanger casing depends on the number of tubes per row, the pitch ratio and the tube outer diameter. Added to this, 0.6 cm separates the last tubes and the sides of the casing (arbitrary value). The height of the on both sides depend on the related thermosiphon part length with 2 cm separating the tube ends from the casing (arbitrary value). Note that there is also an adiabatic layer of height l_a that separates the heat source and heat sink. Finally, the casing length depends on the number of tube rows, the pitch ratio and the tube outer diameter.

$$\begin{aligned}
&\mathrm{W}_{c,e} = 0.012 + S_T\, N_{tpr}\, D_o[m]; \qquad \mathrm{h}_{c,e} = l_e + 0.02\,[m]; \qquad \mathrm{A}_{c,e} = W_{c,e}\, h_{c,e}\,[m^2] \\
&\mathrm{W}_{c,c} = W_{c,e}\,[m]; \qquad\qquad\quad \mathrm{h}_{c,c} = l_c + 0.02\,[m]; \qquad \mathrm{A}_{c,c} = W_{c,c}\, h_{c,c}\,[m^2] \\
&\mathrm{L}_{HTX} = N_{row}\, S_T\, D_o\,[m]
\end{aligned} \tag{32}$$

- The external fluids go through a nozzle divergent before entering the heat exchanger and exit it through a convergent.

- No fins were considered for the sake of code convergence.

- The heat exchanger configuration for both case is counter-flow.This configuration are shown in Figure 5.

  The counter-flow simulation was performed by using the output (target) temperature of the cold fluid and the input temperature of the hot fluid and by simulating each tube as a parallel-flow heat exchanger. The difference is that the heat was removed on both sides of each tube.

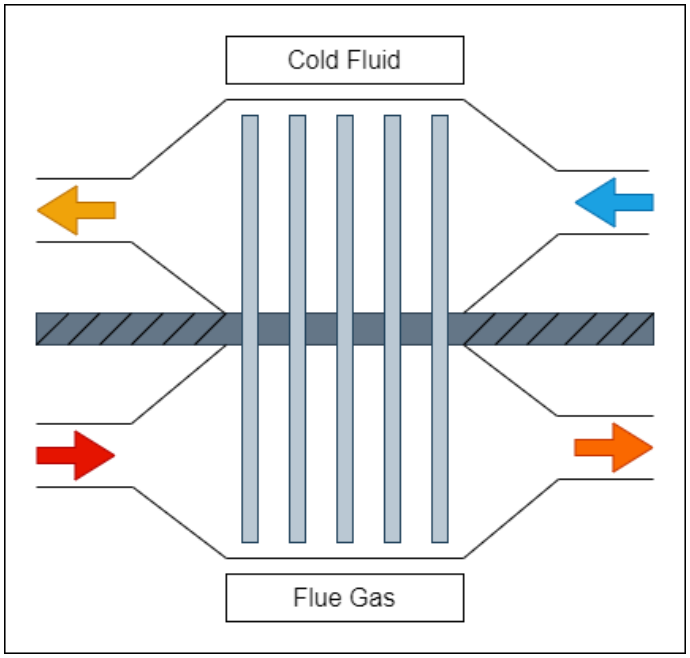

Figure 5: Representation of counter-flow fluid configuration

For the simulation code, a working fluid temperature input can be passed to the model with a range determined by two guesses on the output temperature. The code could fail to converge because of the phase change range of the fluid (especially because of phase change or bad choice of guesses).

5 Possible Future Improvements - Studies

What could be interesting for further study is :

- A dynamic model by introducing some thermal capacities in the model.
- Addition of fins to the heat pipes and a study on their size.
- Integration of direct pool boiling (the functions are already written in the library but not implemented in the general model). There is an *evap_type* parameter in the code for this.
- Generalisation of the pitch ratios to more values by interpolation.
- Improve the pressure loss considerations in the model.

References

[1] *Heat pipes – performance of two-phase closed thermosyphons* - **ESDU 81038**

[2] *Investigation of low Global Warming Potential working fluids for a closed two-phase thermosyphon* - **Robert W. MacGregor , Peter A. Kew , David A. Reay** : https://www.sciencedirect.com/science/article/pii/S1359431112007089

[3] *Perry's chemical engineers' handbook* - **Green DW, Perry RH.**

[4] *Foundations of Heat Transfer* - **Frank P. Incropera, David P. Dewitt, Theodore L. Bergman, Adrienne S. Lavine**

[5] *Tube Banks, Crossflow over* - **Thermopedia** : https://www.thermopedia.com/content/1211/#:~:text=Tube%20banks%20are%20commonly%2Demployed,places%2C%20and%20longitudinal%20flow%20elsewhere